Discovery of bis-sulfonamides as novel inhibitors of mitochondrial NADH-quinone oxidoreductase (complex I)

Atsuhito Tsuji,[1] Takahiro Masuya,[2] Norihito Arichi,[1] Shinsuke Inuki,[1] Masatoshi Murai,[2] Hideto Miyoshi,[2] Hiroaki Ohno*[1]

[1] Graduate School of Pharmaceutical Sciences, Kyoto University, Japan

[2] Division of Applied Life Sciences, Graduate School of Agriculture, Kyoto University, Japan

ABSTRACT: Mitochondrial oxidative phosphorylation (OXPHOS) is an essential cellular metabolic process that generates ATP. The enzymes involved in OXPHOS are considered to be promising druggable targets. Through screening of an in-house synthetic library with bovine heart submitochondrial particles, we identified a unique symmetric bis-sulfonamide (KPYC01112, **1**) as an inhibitor targeting NADH-quinone oxidoreductase (complex I). Structural modifications of KPYC01112 (**1**) led to the discovery of the more potent inhibitors **32** and **35** possessing long alkyl chains (IC_{50} = 0.017 and 0.014 μM, respectively). A photoaffinity labeling experiment using a newly synthesized photoreactive bis-sulfonamide ([^{125}I]-**43**) revealed that it binds to the 49-kDa, PSST, and ND1 subunits, which make up the quinone-accessing cavity of complex I.

KEYWORDS: complex I inhibitor, OXPHOS, bis-sulfonamide, SAR study, mitochondria

Mitochondrial oxidative phosphorylation (OXPHOS) is an essential metabolic process that generates ATP, which in turn, drives various cellular functions. OXPHOS consists of a series of respiratory chain enzymes [NADH-quinone oxidoreductase (complex I), succinate-quinone oxidoreductase (complex II), quinol-cytochrome *c* oxidoreductase (complex III), and cytochrome *c* oxidase (complex IV)], which couple electron transfer to proton translocation across the inner mitochondrial membrane, and F_oF_1-ATP synthase (complex V), which produces ATP driven by the proton gradient (Figure S1). The enzymes involved in OXPHOS are promising targets for the development of pharmaceuticals, antimicrobials, and agrochemicals.[1–6]

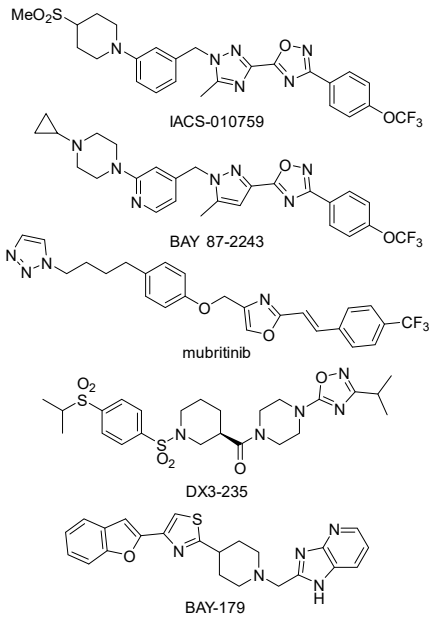

Figure 1. Representative inhibitors of the NADH-quinone oxidoreductase (complex I).

Because OXPHOS inhibitors such as IACS-010759, BAY 87-2243, and mubritinib (Figure 1), all of which target complex I, are anticipated to be candidate compounds for anticancer drugs, screening studies of inhibitors of OXPHOS, particularly complex I, have been extensively conducted. For example, Neamati *et al*. identified a series of benzene-1,4-disulfonamides (including DX3-235) as novel complex I inhibitors from a phenotypic screen using a patient-derived pancreatic cancer cell line (Figure 1).[7,8] The Bayer group identified BAY-179 as a novel complex I inhibitor through an ATP-dependent luciferase reporter assay.[9] We expected that screening of our original compound library using an enzyme-based assay would lead to the identification of novel inhibitors of the respiratory chain enzymes with an unprecedented mode of action and/or structural framework. In the present study, we identified a unique symmetric bis-sulfonamide (KPYC01112, **1**, Figure 2) as an inhibitor targeting bovine mitochondrial complex I. Structural modifications of this compound led to more potent derivatives. Photoaffinity labeling experiments showed that these bis-sulfonamides bind to the 49-kDa, PSST, and ND1 subunits, which make up the quinone-accessing cavity of complex I.

Compound library screening. To find novel inhibitors of the mitochondrial respiratory enzymes, we selected 107 low-molecular-weight compounds with diverse scaffolds from our in-house compound library, consisting of the originally synthesized compounds with unique structures. Using submitochondrial particles (SMPs) prepared from bovine heart mitochondria, evaluation of their inhibitory activities against NADH oxidase activity (covering complexes I, III, and IV activities) resulted in 12 hit compounds showing <30% residual activity at 5 μM (Figure S2). Through evaluation of the concentration dependency, we identified the most potent compound KPYC01112 (**1**) (IC_{50} = 0.87 μM, Figure 2). This compound was previously synthesized by Ibuka *et al*. in their study of aza-Payne rearrangement,[10] where its biological activity was not reported. Therefore, we subjected KPYC01112 to a SAR study focusing on ring size,

stereochemistry, structural symmetricity, junction part, and the sulfonamide moiety to improve its inhibitory activity.

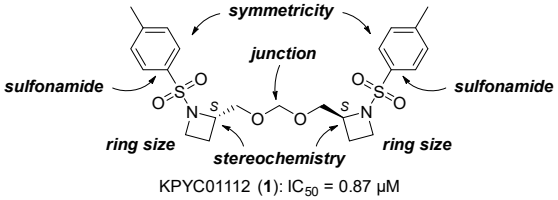

Figure 2. The structure of KPYC01112 (**1**) and the structure optimization strategy.

A typical synthesis of the KPYC01112 derivatives is shown in Scheme 1. The dimeric methylene acetal moiety was constructed in accordance with the method reported by Ibuka *et al*.[10] Thus, treatment of alcohol **2** (2 equiv.) with *t*-BuOK in CH_2Cl_2 gave the methylene acetal **3** in 41% yield. Hetero-coupling of non-identical alcohols was performed according to Undheim *et al*.[11] Methylthiomethylation of **4** via the Pummerer rearrangement with dimethyl sulfoxide in the presence of acetic acid and acetic anhydride[12] followed by chlorination using sulfuryl chloride gave the chloromethyl ether **5**. The hetero-dimer **6** was obtained by coupling of **5** with the stereoisomeric alcohol *ent*-**4**. Other KPYC01112 derivatives were synthesized in a similar manner (see Supporting Information).

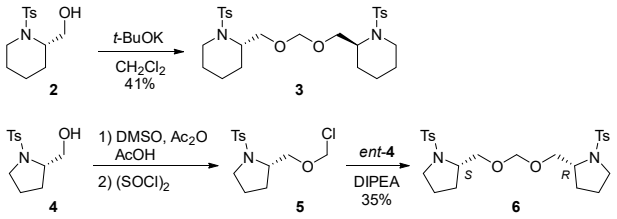

Scheme 1. Synthesis of the KPYC01112 derivatives.

Ring size and stereochemistry. The synthesized KPYC01112 derivatives were evaluated for their inhibition of NADH oxidase activity in SMPs as conducted in the library screening above. The pyrrolidine derivative **7** maintained the inhibitory activity (IC_{50} = 0.89 μM), whereas the piperidine derivative **3** showed decreased inhibitory activity (IC_{50} = 2.6 μM). Similarly, the cyclohexane-fused pyrrolidine **8** and methylamine derivative **9** lacking the ring structure exhibited significantly lower inhibitory activity (IC_{50} = 5.8 μM and 6.4 μM, respectively). From these results, the azetidine and pyrrolidine derivatives were deemed to be suitable for the inhibition of NADH oxidase activity. Further structural optimization of the pyrrolidine derivatives was performed because of the availability of the starting materials and ease of synthesis.

To estimate the relationship between the stereochemistry and the enzyme inhibitory activity, we evaluated the activity of *ent*-**7** and **6** having the (*R*,*R*)- and (*S*,*R*)-configuration, respectively. The inhibitory activity of the *meso*-derivative **6** (IC_{50} = 0.81 μM) was comparable to the parent compound **7** (IC_{50} = 0.89 μM), while the activity of *ent*-**7** (IC_{50} = 3.1 μM) was decreased to one-fifth that of **7**. These results suggested that at least one of the stereocenters should be *S* to interact with the target molecule(s). The monomeric alcohol **4** was almost inactive (IC_{50} >230 μM), indicating the importance of the dimeric and/or acetal structure.

Table 1. Structure-activity relationship of the KPYC01112 derivatives.[a]

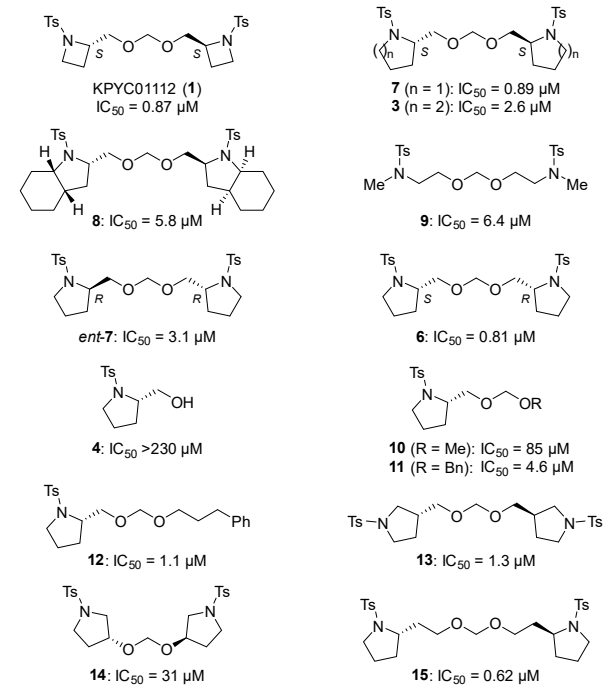

[a] IC_{50} values are the molar concentrations needed to reduce the control NADH oxidase activity in SMPs by 50%. Data shown are average values of at least two independent measurements.

Symmetricity and junction part. KPYC01112 (**1**) and the pyrrolidine congener **7** have a characteristic symmetrical acetal structure where the two *N*-heterocycles are connected to each other at the 2-position. Thus, we next investigated the unsymmetrical acetals as well as the symmetric dimers connected at the different position. The unsymmetrical acetal derivatives **10** (R = Me; IC_{50} = 85 μM), **11** (R = Bn; IC_{50} = 4.6 μM), and **12** [R = $(CH_2)_3$Ph; IC_{50} = 1.1 μM], in which one ring structure was replaced by an alkyl group, tend to be all less potent inhibitors than **7**. Among these substituents, the larger structures are more active, with compound **12** having a 3-phenylpropyl group showing an activity close to **7**. Dimeric pyrrolidine **13** connected at the pyrrolidine 3-position showed approximately the same activity (IC_{50} = 1.3 μM) as **7**. A lower inhibitory activity was observed with derivative **14** (IC_{50} = 31 μM), where the number of atoms between *N* and *N′* was seven as in derivative **7**. By comparison, homoprolinol-type compound **15**, bearing a one-carbon-longer tether connected at the 2-position showed comparable inhibitory activity (IC_{50} = 0.62 μM) to that of **7**. These results indicate that the linkage of the pyrrolidine rings at the 2-position is important, although the linker length has some flexibility.

Sulfonamide moiety. Next, we proceeded to investigate the sulfonamide moiety (Table 2). Because the amide **16** was less active (IC_{50} = 5.0 μM), we focused on the derivatization of the sulfonamides. The activities of benzenesulfonamides **17** (R = H) and **18** (R = OMe) with a different substitution pattern at the

para position were less effective (IC_{50} = 4.1 and 4.4 μM, respectively), while **19** (R = Cl) showed nearly equal activity (IC_{50} = 1.1 μM) to **7**. Introduction of a longer carbon chain at the para position showed an interesting tendency: *n*-butyl (**20**) and *n*-pentyl (**21**) derivatives exhibited *ca*. 6-fold more potent inhibitory activity (IC_{50} = 0.14 and 0.15 μM, respectively) than **7**, and the activity was maximal when the carbon chain length was six (**22**, IC_{50} = 0.098 μM). On the other hand, the inhibitory activities of the *n*-heptyl (**23**) and *n*-octyl (**24**) derivatives were relatively poor (IC_{50} = 3.6 and 3.4 μM, respectively). Furthermore, the benzene ring of the sulfonamide was not essential: among the sulfonamides **25**–**27** having a C8, C10, or C12 linear alkyl group, the 1-decanesulfonamide **26** showed the most potent inhibitory activity (IC_{50} = 0.088 μM). It is worth noting that the optimized benzenesulfonamide **22** (*n*-hexylphenyl) and alkanesulfonamide **26** (*n*-decanyl) have a similar carbon chain length.

Table 2. Investigation of the sulfonamide moiety.[a]

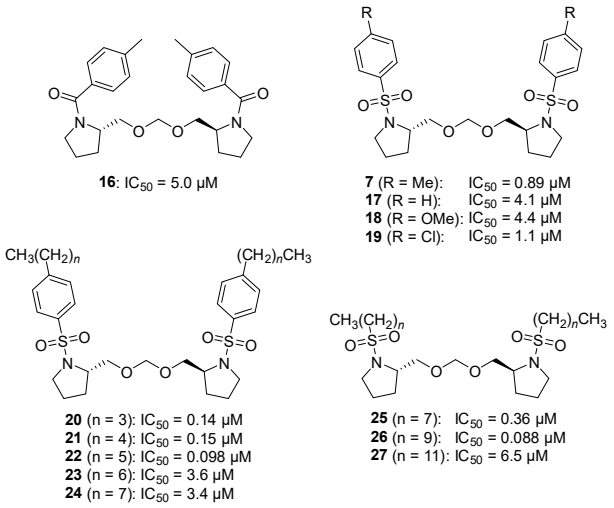

[a] IC_{50} values are the molar concentrations needed to reduce the control NADH oxidase activity in SMPs by 50%. Data are average values of at least two independent measurements.

Further structural optimization of the long-chain alkyl group was performed (Table 3). Introduction of an oxygen atom to the alkyl chain slightly increased the inhibitory activity by approximately 1.8-fold (**28**, IC_{50} = 0.048 μM), while introduction of two oxygen atoms slightly decreased the activity (**29**, IC_{50} = 0.26 μM). By using the oxygen atom in the alkyl group, we investigated the introduction of an aromatic ring with a view to probe the synthesis. Among the phenyl ethers having a phenyl, tolyl, or *para*-iodophenyl group(s) (**30**–**35**), the *para*-iodophenyl derivatives **32** and **35** showed good inhibitory activity (IC_{50} = 0.017 and 0.014 μM, respectively). Interestingly, analogs **32** and **35** showed almost the same activities, although the other oxygen-containing symmetrical analogs (**29**, **33** and **34**) showed weaker activities than the corresponding asymmetrical ones (**28**, **30** and **31**, respectively). This can be attributed to the hydrophobic effect of the *para*-iodophenyl group, which could cancel the negative effect of the second oxygen atom in **35**. Thus, we identified 3-(aryloxy)propanesulfonamides **32** and **35** having approximately 60-fold more potent inhibitory activity compared with compound **1**.

Table 3. Investigation of the alkanesulfonamides.[a]

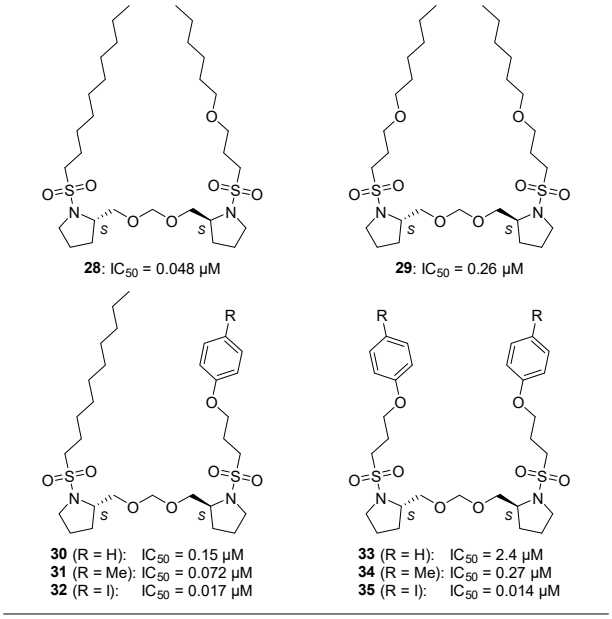

[a] IC_{50} values are the molar concentrations needed to reduce the control NADH oxidase activity in SMPs by 50%. Data are average values of at least two independent measurements.

Investigation of the target enzyme. The target enzyme(s) of compounds **32** and **35**, which showed the most potent inhibitory activity, was investigated. The NADH-Q_1 oxidoreductase activity (only complex I activity) was significantly inhibited by **32** and **35** (IC_{50} = 0.040 and 0.026 μM, respectively), whereas the succinate-cytochrome *c* oxidoreductase activity (covering complexes II and III activities) was not blocked [IC_{50} >20 μM, (Table 4)]. These results indicate that the target enzyme of these compounds is complex I. To exclude the possibility that the apparent inhibition is related to some nonspecific disturbance of the lipid bilayer phase of SMPs, we checked the effects of **1**, **32**, and **35** on the formation of the membrane potential in SMPs driven by ATP hydrolysis. The addition of **1**, **32**, or **35** to SMPs did not attenuate the membrane potential (Figure S3), implying that these compounds specifically inhibit complex I among the respiratory enzymes.

Table 4. Identification of the enzyme targeted by the inhibitors.

	IC_{50} (μM)[a]	
	NADH-Q_1	succinate-cytochrome *c*
32	0.040	>20
35	0.026	>20

[a] IC_{50} values are the molar concentrations needed to reduce the control NADH-Q_1 oxidoreductase activity or succinate-cytochrome *c* oxidoreductase activity in SMPs by 50%. Data are average values of at least two independent measurements.

To identify the binding site in complex I, we designed a photoreactive derivative [^{125}I]-**43** based on **32**, which has a diazirine ring and ^{125}I as a photoreactive group and detection tag, respectively. As shown in Scheme 2, sulfonylation of the known protected prolinol **36** with **37** followed by diazirine formation as reported by Abe *et al.*[13] and desilylation gave diazirine alcohol **40**. By comparison, sulfonylation of **36** with sulfonyl chloride **41** bearing an iodophenoxy group and removal of the silyl group afforded **42**. Dimeric acetal formation of **40** and **42** using dichloromethane in the presence of *t*-BuOK gave **43**, which was converted to the ^{125}I-labeled derivative via tributylstannylation.[14] The inhibitory activity of the cold compound **43** (IC_{50} = 0.016 μM) against the NADH oxidase activity was comparable to the parent compound **32** (IC_{50} = 0.017 μM).

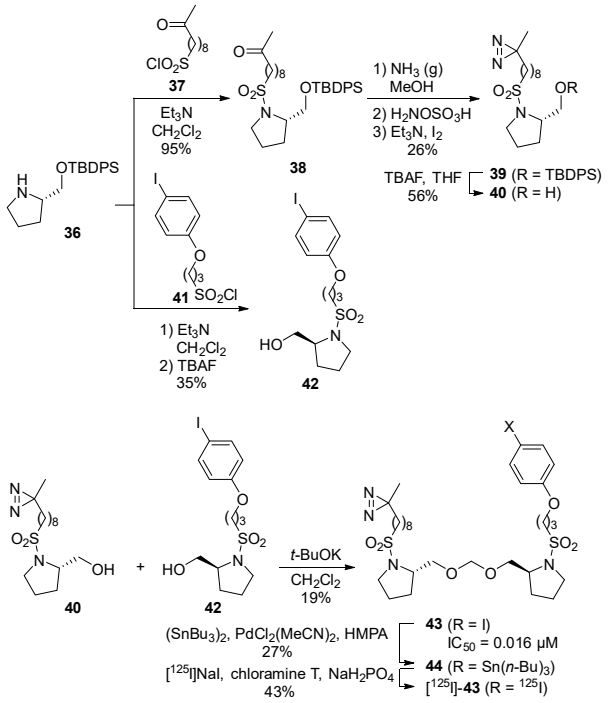

Scheme 2. Synthesis of the ^{125}I-labeled probe [^{125}I]-**43**.

Using [^{125}I]-**43**, we conducted photoaffinity labeling experiments to identify its binding subunit(s) in complex I. After bovine heart SMPs were labeled with [^{125}I]-**43**, the labeled complex I was isolated by Blue Native PAGE (BN-PAGE) and separated by doubled SDS-PAGE. [^{125}I]-**43** primarily labeled the 49-kDa, ND1, and PSST subunits in complex I (Figure 3A, Figure S4). These three subunits make up the canonical quinone-accessing cavity of complex I (Figure 3B).[15–17] Therefore, it is likely that [^{125}I]-**43** binds to the cavity or around the cavity.

Next, the effects of using an excess of other inhibitors on the labeling by [^{125}I]-**43** (5 nM) were investigated by a competition test (5 μM, 1000-fold molar excess). Here we used a cold form of **43**, the parent compounds **32** and **35**, and the known "quinone site" inhibitors bullatacin and aminoquinazoline (AQ). These competitors significantly suppressed the labeling by [^{125}I]-**43** (Figure 4). These results strongly suggest that compounds **32** and **35** also bind to the quinone-accessing cavity or around the cavity.

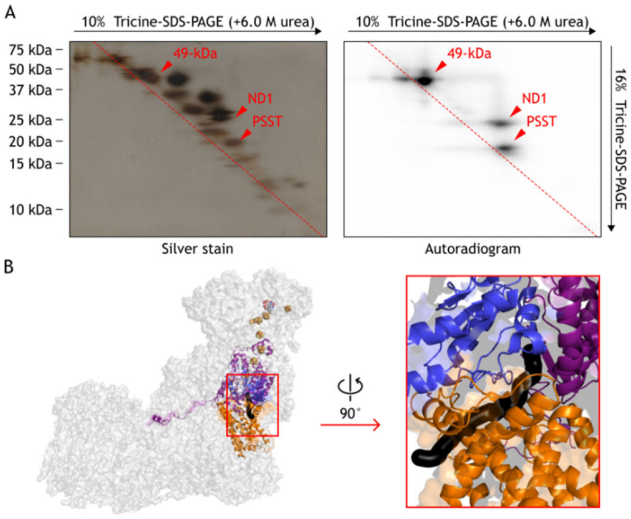

Figure 3. Photoaffinity labeling of complex I by [^{125}I]-**43**. (A) SMPs (4.0 mg of protein/mL) were labeled by [^{125}I]-**43** (10 nM), followed by the purification of complex I by BN-PAGE and electroelution. The isolated complex I was resolved by doubled SDS-PAGE, and the SDS gel was subjected to silver staining or autoradiography. (B) The subunits labeled by [^{125}I]-**43** in bovine complex I. The 49-kDa (*pink*), ND1 (*orange*), and PSST (*blue*) subunits in complex I (PDB ID: 5O31)[18] are shown. The quinone-accessing cavity is formed at the interface of the 49-kDa, ND1, and PSST subunits as indicated by a *black sphere* generated using MOLE with a 1.4-Å probe (https://mole.upol.cz).[19]

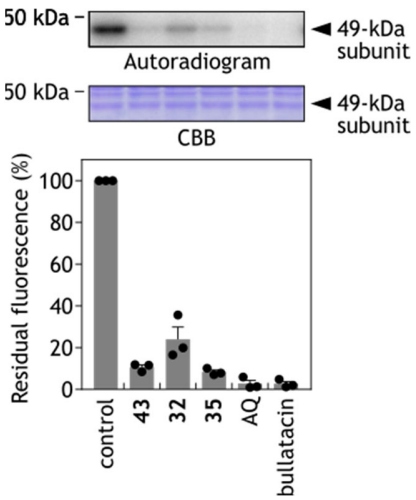

Figure 4. Effects of various inhibitors (i.e., competitors) on the specific binding of [^{125}I]-**43** to the 49-kDa subunit.

In conclusion, through the screening of an in-house library, we identified KPYC01112 (**1**) possessing a unique framework as a specific inhibitor of mitochondrial complex I. Structural optimization based on a SAR study produced novel sulfonamide derivatives **32** and **35**, which are approximately 60-fold more potent than the parent KPYC01112. The photoaffinity labeling experiments indicated that the sulfonamide derivatives bind the quinone-accessing cavity or around the cavity in complex I.

ASSOCIATED CONTENT

Supporting Information

The Supporting Information is available free of charge on the ACS Publications website.

Supplementary figures S1–S5; biological assay protocols, synthetic experimental details, characterization data (PDF)

AUTHOR INFORMATION

Corresponding Author

Hiroaki Ohno – Graduate School of Pharmaceutical Sciences, Kyoto University

Authors

Atsuhito Tsuji – Graduate School of Pharmaceutical Sciences, Kyoto University

Takahiro Masuya – Division of Applied Life Sciences, Graduate School of Agriculture, Kyoto University

Norihito Arichi – Graduate School of Pharmaceutical Sciences, Kyoto University

Shinsuke Inuki – Graduate School of Pharmaceutical Sciences, Kyoto University

Masatoshi Murai – Division of Applied Life Sciences, Graduate School of Agriculture, Kyoto University

Hideto Miyoshi – Division of Applied Life Sciences, Graduate School of Agriculture, Kyoto University

Author Contributions

Atsuhito Tsuji conducted all the experiments under the guidance of Hiroaki Ohno, Shinsuke Inuki, and Norihito Arichi (for the synthetic and medicinal chemistry study), and Hideto Miyoshi, Takahiro Masuya, and Masatoshi Murai (for the biochemical study). The manuscript was written with contributions from all authors. All authors have approved the final version of the manuscript.

ACKNOWLEDGMENT

This work was supported by the JSPS KAKENHI (grant numbers 22J15893, 22K19028, 21H02130, 22K14837, and 22H02273), AMED (grant number JP19gm1010007), the Research Support Project for Life Science and Drug Discovery [Basis for Supporting Innovative Drug Discovery and Life Science Research (BINDS)] from AMED (grant numbers JP22ama121034 and JP22ama121042), and the Naito Foundation. The experiments involving radioisotope techniques were performed at the Radioisotope Research Center, Kyoto University.

ABBREVIATIONS

OXPHOS, oxidative phosphorylation; complex I, proton-translocating NADH-quinone oxidoreductase; NADH, nicotinamide adenine dinucleotide, reduced form; complex II, succinate dehydrogenase; complex III, quinol-cytochrome *c* oxidoreductase; complex IV, cytochrome *c* oxidase; complex V, FoF1-ATPsynthase; SMP, submitochondrial particle; SAR, structure-activity relationship; *t*-BuOK, potassium *tert*-butoxide; Q_1, 2,3-dimethoxy-5-methyl-6-(3-methyl-2-buten-1-yl)-2,5-cyclohexadiene-1,4-dione; PAGE, polyacrylamide gel electrophoresis; BN-PAGE, Blue Native PAGE; SDS-PAGE, sodium dodecyl sulfate PAGE; AQ, 6-amino-4-(4-*tert*-butylphenetylamino)quinazoline.

REFERENCES

(1) Xu, Y.; Xue, D.; Bankhead, A.; Neamati, N. Why All the Fuss about Oxidative Phosphorylation (OXPHOS)? *J. Med. Chem.* **2020**, *63*, 14276–14307. https://doi.org/10.1021/acs.jmedchem.0c01013

(2) Carter, J. L.; Hege, K.; Kalpage, H. A.; Edwards, H.; Hüttemann, M.; Taub, J. W.; Ge, Y. Targeting Mitochondrial Respiration for the Treatment of Acute Myeloid Leukemia. *Biochem. Pharmacol.* **2020**, *182*, 114253. https://doi.org/10.1016/j.bcp.2020.114253

(3) Carter, J. L.; Hege, K.; Yang, J.; Kalpage, H. A.; Su, Y.; Edwards, H.; Hüttemann, M.; Taub, J. W.; Ge, Y. Targeting Multiple Signaling Pathways: The New Approach to Acute Myeloid Leukemia Therapy. *Signal Transduct. Target Ther.* **2020**, *5*, 288. https://doi.org/10.1038/s41392-020-00361-x

(4) van Gisbergen, M. W.; Zwilling, E.; Dubois, L. J. Metabolic Rewiring in Radiation Oncology Toward Improving the Therapeutic Ratio. *Front. Oncol.* **2021**, *11*, 653621. https://doi.org/10.3389/fonc.2021.653621

(5) Tan, Y. Q.; Zhang, X.; Zhang, S.; Zhu, T.; Garg, M.; Lobie, P. E.; Pandey, V. Mitochondria: The Metabolic Switch of Cellular Oncogenic Transformation. *Biochim. Biophys. Acta Rev. Cancer* **2021**, *1876*, 188534. https://doi.org/10.1016/j.bbcan.2021.188534

(6) Bueno, M. J.; Ruiz-Sepulveda, J. L.; Quintela-Fandino, M. Mitochondrial Inhibition: A Treatment Strategy in Cancer? *Curr. Oncol. Rep.* **2021**, *23*, 49. https://doi.org/10.1007/s11912-021-01033-x

(7) Xue, D.; Xu, Y.; Kyani, A.; Roy, J.; Dai, L.; Sun, D.; Neamati, N. Discovery and Lead Optimization of Benzene-1,4-Disulfonamides as Oxidative Phosphorylation Inhibitors. *J. Med. Chem.* **2022**, *65*, 343–368. https://doi.org/10.1021/acs.jmedchem.1c01509

(8) Xue, D.; Xu, Y.; Kyani, A.; Roy, J.; Dai, L.; Sun, D.; Neamati, N. Multiparameter Optimization of Oxidative Phosphorylation Inhibitors for the Treatment of Pancreatic Cancer. *J. Med. Chem.* **2022**, *65*, 3404–3419. https://doi.org/10.1021/acs.jmedchem.1c01934

(9) Mowat, J.; Ehrmann, A. H. M.; Christian, S.; Sperl, C.; Menz, S.; Günther, J.; Hillig, R. C.; Bauser, M.; Schwede, W. Identification of the Highly Active, Species Cross-Reactive Complex I Inhibitor BAY-179. *ACS Med. Chem. Lett.* **2022**, *13*, 348–357. https://doi.org/10.1021/acsmedchemlett.1c00666

(10) Ibuka, T.; Nakai, K.; Habashita, H.; Hotta, Y.; Otaka, A.; Tamamura, H.; Fujii, N.; Mimura, N.; Miwa, Y.; Chounan, Y.; Yamamoto, Y. Aza-Payne Rearrangement of Activated 2-Aziridinemethanols and 2,3-Epoxy Amines under Basic Conditions. *J. Org. Chem.* **1995**, *60*, 2044–2058. https://doi.org/10.1021/jo00112a028

(11) Benneche, T.; Strande, P.; Undheim, K. A New Synthesis of Chloromethyl Benzyl Ethers. *Synthesis* **1983**, 762–763. https://doi.org/10.1055/s-1983-30506

(12) Yamada, K.; Kato, K.; Nagase, H.; Hirata, Y. Protection of Tertiary Hydroxyl Groups as Methylthiomethyl Ethers. *Tetrahedron Lett.* **1976**, *17*, 65–66. https://doi.org/10.1016/S0040-4039(00)71324-4

(13) Abe, M.; Nakano, M.; Kosaka, A.; Miyoshi, H. Syntheses of Photoreactive Cardiolipins for a Photoaffinity Labeling Study. *Tetrahedron Lett.* **2015**, *56*, 2258–2261. https://doi.org/10.1016/j.tetlet.2015.03.056

(14) Murai, M.; Ishihara, A.; Nishioka, T.; Yagi, T.; Miyoshi, H. The ND1 Subunit Constructs the Inhibitor Binding Domain in Bovine Heart Mitochondrial Complex I. *Biochemistry* **2007**, *46*, 6409–6416. https://doi.org/10.1021/bi7003697

(15) Baradaran, R.; Berrisford, J. M.; Minhas, G. S.; Sazanov, L. A. Crystal Structure of the Entire Respiratory Complex I. *Nature* **2013**, *494*, 443–448. https://doi.org/10.1038/nature11871

(16) Zickermann, V.; Wirth, C.; Nasiri, H.; Siegmund, K.; Schwalbe, H.; Hunte, C.; Brandt, U. Mechanistic Insight from the Crystal Structure of Mitochondrial Complex I. *Science* **2015**, *347*, 44–49. https://doi.org/10.1126/science.1259859

(17) Zhu, J.; Vinothkumar, K. R.; Hirst, J. Structure of Mammalian Respiratory Complex I. *Nature* **2016**, *536*, 354–358. https://doi.org/10.1038/nature19095

(18) Blaza, J. N.; Vinothkumar, K. R.; Hirst, J. Structure of the Deactive State of Mammalian Respiratory Complex I. *Structure* **2018**, *26*, 312–319. https://doi.org/10.1016/j.str.2017.12.014

(19) Pravda, L.; Sehnal, D.; Toušek, D.; Navrátilová, V.; Bazgier, V.; Berka, K.; Svobodová Vařeková, R.; Koča, J.; Otyepka, M. MOLEonline: A Web-Based Tool for Analyzing Channels, Tunnels and Pores. *Nucleic Acids Res.* **2018**, *46*, W368–W373. https://doi.org/10.1093/nar/gky309

TOC Graphic

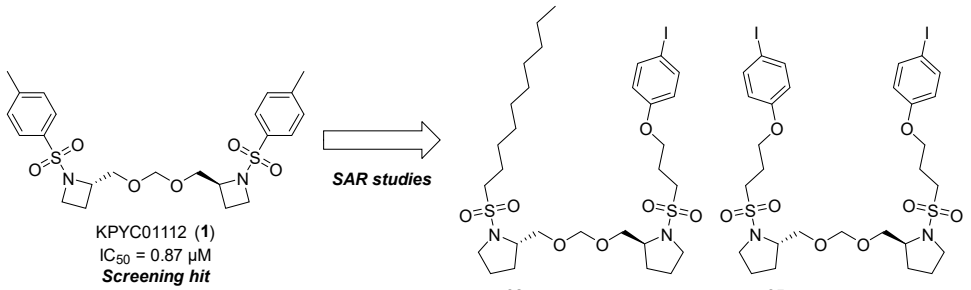

KPYC01112 (**1**)
IC_{50} = 0.87 μM
Screening hit

32: IC_{50} = 0.017 μM

35: IC_{50} = 0.014 μM